atoms

MDPI

Article

Ni- and Co-like Xe Ion EUV Spectra Produced by Excitation Around the Ionisation Threshold of Xe XXVII

Elmar Träbert [1,2]

[1] AIRUB, Fakultät für Physik und Astronomie, Ruhr-Universität Bochum, 44780 Bochum, Germany; traebert@astro.rub.de
[2] Physics Division, Lawrence Livermore National Laboratory, Livermore, CA 94550-9234, USA

Abstract

A high-resolution flat-field grating spectrometer has been employed at the Livermore EBIT-I electron beam ion trap for observations of extreme-uv spectra of Ni-like ions Xe^{26+} and Co-like ions Xe^{27+}. Multistep ionisation involving the long-lived $3d^9 4s\ ^3D_3$ level in the Ni-like ion as a stepping stone has a significant influence on the charge state distribution at a given electron beam energy, as has been reported elsewhere. Complementing those observations of 3d-4s *E*2 and *M*3 transitions from long-lived levels, the present report shows spectra of 3d-4p and 3d-4f *E*1 transitions that arise from the decays of short-lived levels in both ions and their neighbouring ions of higher charge states and provide bright reference signals for the changes in the charge state distribution. Their observation is serendipitously furthered by the visual absence of 3d-4d transitions from the observed spectra, although *M*1 and *E*2 transitions between these configurations are permitted.

Keywords: highly charged ions; extreme-ultraviolet spectra; electron beam ion trap; metastable level; charge state distribution; electric dipole selection rules; multipole order

1. Introduction

For many dilute plasmas, the (usually Maxwellian) energy distribution of the electrons is used to predict the charge state distribution of the ions. This is because electron-ion collisions lead to ion excitation and ionisation. Many calculations (in the low-density approximation) assume that a given excited ion has time enough to return to the ground state before it is being hit by another energetic electron. Hence only ground state ions are considered as targets, and then only the binding energy of the ground state matters in judging whether an electron has sufficient energy to ionise the target. Moreover, at a given temperature, a Maxwellian electron energy distribution comprises low-energy electrons that cannot excite any level in a highly charged ion, and high-energy electrons that may surpass most excitation thresholds even in a relatively cool plasma, so that the actual excitation energies of many levels do matter little in terms of the ionisation balance or charge state distribution. For example, the laboratory spectroscopy of specific elements purportedly began with the observation of the sodium "D" lines that appeared when sprinkling table salt into a flame. We nowadays know that such a flame in ambient air has a temperature on the order of 1000 K or 1/10 eV, whereas the excitation energy of the Na I 3p levels, the upper levels of the sodium resonance lines, amounts to roughly 2 eV. Without the high-energy tail of the Maxwellian electron energy distribution, Na atoms would not be excited in a flame.

Check for updates

Received: 29 December 2025
Revised: 10 March 2026
Accepted: 11 March 2026
Published: 12 March 2026

Electron-collision calculations (collisional-radiative models, CR) for describing a plasma may be challenged by the presence of metastable levels. An example of such a long-lived excited level in highly charged Ni-like ions is the $3d^9 4s\ ^3D_3$ level that decays to the $3d^{10}\ ^1S_0$ ground state only by a magnetic octupole ($M3$) transition (as was first observed in the spectra of Ni-like ions of thorium (Z = 90) and uranium (Z = 92) [1]). Such a high-multipole order radiative transition has a much lower transition probability than $E1$, $M1$, or $E2$ transitions between comparable electron configurations. The role of this level may be elucidated by using a quasi-mono-energetic electron beam as is available in an electron beam ion trap, where a variation of the electron beam energy may probe the threshold range for ionisation with or without involving the long-lived excited level.

The Livermore EBIT group has reported energy and lifetime measurements on this level for Ni-like ions of Xe (Z = 54), Cs (Z = 55), and Ba (Z = 56) (in natural isotope mixtures) [2] and studied the influence of hyperfine mixing on the long (millisecond-range) $3d^9 4s\ ^3D_3$ level lifetime in Xe isotopes with a non-zero nuclear spin [3]. The measurements employed an electron beam ion trap, a high-resolution flat-field EUV grating spectrograph [4], and a microcalorimeter [5–7]. This experimental research and its supportive theoretical effort (involving CR) has elucidated the atomic physics setting as well as yielded tools for plasma diagnostics. The multi-step ionisation process has been noted in other and similar contexts by others as well (see [7] and the citations therein). That discussion does not need to be repeated here.

The Livermore EBIT group studies of the Ni- and Co-like ions (and recent studies of similar systems by others) yield quite some information beyond those metastable levels. For example, in the range of the EUV spectrum adjacent to the 3d-4s transitions, there are 3d-4p and 3d-4f transitions (see [5,7–9]). Their upper levels are short-lived, because these transitions are of the $E1$ multipole order with transition rates many orders of magnitude higher than those of the higher-multipole order decays ($E2$, $M3$) of the metastable levels. The line ratios involving $E1$ transitions thus do not need an ion trap environment for ion production and might be helpful also for the study of transient plasmas and the charge state distributions therein.

The study of $E1$ transitions in the investigation of charge state distributions is not new, of course. Incidentally we have recognised that the seeming absence of 3d-4d transitions from the EUV spectra of Ni-like (and neighbouring) ions yields a spectral window generated by the schematics of atomic selection rules, which divert the level population to decay channels in another spectral range. Thus a different set of transitions can be seen in specific experimental settings. There is no new physics effect involved. In hindsight, the phenomenon could have been deduced from looking at large tables of computed rates for transitions of various multipole orders, or from a bit of educated thinking, but apparently it was not.

2. Experiment

The experiment was done at the University of California Lawrence Livermore National Laboratory EBIT-I low-energy electron beam ion trap [10] which operates at a 3 T magnetic field provided by crogenically cooled superconducting coils. Most of the present work was done at electron beam energies near 1500 eV, that is, just below and above the ionisation potential of Xe^{26+} at 1493 ± 4 eV [11], and at electron beam currents from 1 mA up to about 40 mA. (Ionisation potentials have been published variously, and many can also be obtained from spectroscopic databases.) The electron beam is quasi-monoenergetic, with an energy spread on the order of 50 eV.

Xe gas was continually injected into the trap volume from a reservoir at a pressure of up to 10^{-6} Pa. Based on previous experience, this makes for a gas pressure in the center of the injected gas plume that is on the order of 10^{-8} Pa, compared to an ambient pressure in the ion trap that is another two orders of magnitude lower. The process of always breeding from neutral atoms provides for a charge state distribution that comprises all charge states up to the maximum. The time development of the charge state distribution could be monitored by means of a microcalorimeter [12–14] observing the X-ray spectrum up to several keV photon energy.

For high-resolution EUV spectroscopy, a flat-field grazing incidence spectrometer was used that was equipped with a gold-coated variable line spacing grating of R = 44.3 m radius of curvature and 2400 ℓ/mm average groove density, set up at an angle of incidence of about 88° [4]. The associated detector comprised a cryogenically cooled thinned back-illuminated charge-coupled device (CCD) of 1350 × 1300 pixels on a 25 mm × 25 mm substrate. Typical exposure times were 20 to 30 min.

The wavelength coverage varies with the mean wavelength setting of the spectrograph; it is about 7 Å in our range of interest. Each pixel then corresponds to a wavelength interval of about 5.4 mÅ. As we image the electron beam with about unity magnification onto the detector, the typical line width is about five pixels, or 27 mÅ, and the resolving power is about 800 for wavelengths near 20 Å (photon energy ≈ 600 eV). The wavelength scale has been converted to an energy scale. On this scale, the line width changes markedly between the low and high energy ends of the spectral range covered in the figures. However, the regularity of the *Z*-scaling of the excitation energies is better seen in this representation.

The prominent Xe lines of interest are close to the resonance lines of He-like O VII and H-like O VIII which served as wavelength references [5]. The lines discussed here mostly lie beyond the wavelength/energy range discussed there and require some extrapolation of the wavelength scale. However, the present data show several peculiar phenomena, and for this illustrative exploration an extension of the previously established scale seems good enough.

3. Electronic Structure

Atomic structure systematics based on quantum mechanic principles have been established a century ago, beginning with single-electron atoms (hydrogen) and explaining the structure of many-electron systems sufficiently well within a decade. The selection rules for transitions in atomic systems with reference to parity and total angular momentum are sufficient to discuss the present study objects and spectral observations. For the data to discuss, the underlying principles are easiest to show for Ni-like ions (see Figure 1), although the same rules apply to Co-like and corresponding ions, of course.

In Ni-like ions, the ground configuration has a closed $3d^{10}$ shell, and the ground state has a term designation of $^1S_0$. The first excited configuration is $3d^9 4s$, with $^1D_2$ and $^3D_{1,2,3}$ levels. For these levels to decay, the 4s electron (in a single-electron picture) has to turn into a 3d electron, which involves a change of angular momentum quantum number ℓ by two units, while parity does not change. In short, for the $3d^9 4s$ levels, 3d-4s transitions are strictly $E1$-forbidden. $M1$ transitions from the $J = 1$ level connect to the ground state and to the excited $J = 2$ level, $E2$ decays of the $J = 2$ level lead to the ground state, the $M3$ decay of the $J = 3$ level goes to the ground state as well. The upper-level lifetimes have been discussed and partly measured [2,3].

$3d^9 4p$ levels: A 3d-4p $E1$ decay is allowed for $J = 1$ levels to proceed to the $3d^{10}$ ground state, as well as (for levels of various J values) by an 4s-4p $E1$ transition to $3d^9 4s$ levels. 4s and 4p levels as well as 3d-4p transitions in Ni- and Co-like ions of Xe have been treated computationally in [5].

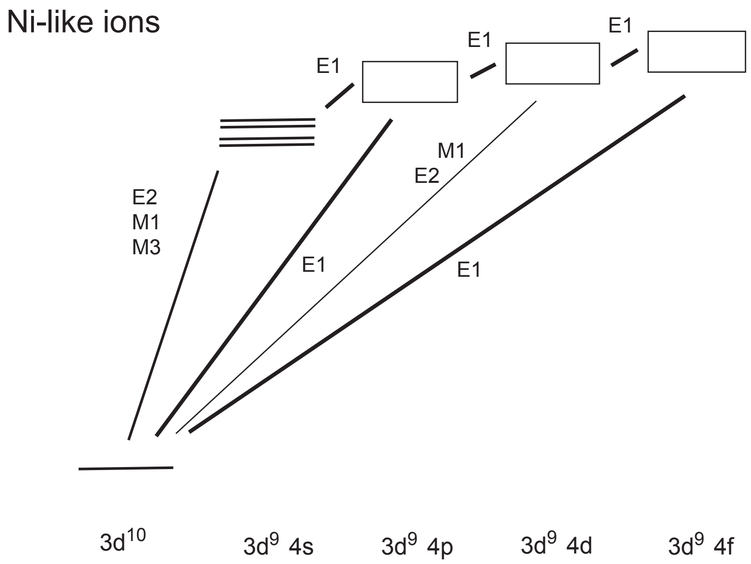

Figure 1. Schematic of $3d^{10}$ and $3d^9 4l$ levels and transitions among them (Excitation energies not to scale). The many $3d^9 4p$, $3d^9 4d$, and $3d^9 4f$ levels are represented by boxes. Along the lines indicating the numerous transitions, the multipole orders of the dominant decay branches are indicated.

$3d^9 4d$ levels: Because of parity there can be no 3d-4d $E1$ transitions to the ground state. $M1$ and $E2$ transitions are possible and have been computed in the literature for the $3d^{10}$-$3d^9 4\ell$ transition arrays. However, no such transitions have been observed yet. This is probably due to just the lower rate of higher multipole order transitions compared to the 4p-4d $E1$ transitions.

$3d^9 4f$ levels: The 4f levels have wave functions that are largely located outside of the 3d electron core, so that among the 4ℓ levels the 4f levels come closest in energy to the hydrogenic case of a single electron outside of a screened nuclear Coulomb field. Such "yrast" transitions between levels of maximum angular momentum ℓ collect much of the cascade repopulation from higher-lying levels, and consequently they are prominent in many plasmas (for an example, see [15]). Various 3d-4f $E1$ transitions to the $3d^{10}$ ground state are allowed for 4f levels with $J = 1$, but there are also 4d-4f $E1$ intra-shell decay channels for many 4f levels.

In Ni-like ions with one electron excited, there is a $3d^9$ electron core with rather few terms. In Co-like ions, with one electron excited, the $3d^8$ core offers many more levels. The difference is seen in Figure 2, where the Ni-like spectra are dominated by a few lines, while the Co-like spectra feature more, individually weaker lines spread out over a certain energy interval.

Spectra in a comparable energy range and electron beam energy variation, but obtained with a microcalorimeter, have also recently been reported from the NIST Gaithersburg EBIT [8,9]. Those publications show Gd ($Z = 59$) and Nd ($Z = 60$) spectra, respectively, at a slightly poorer resolution than the present grating spectrometer observations of Xe ions. The spectra comprise the 3d-4s, 3d-4p, and 3d-4f transitions, but appear to avoid observations of higher charge state ions as are discussed below.

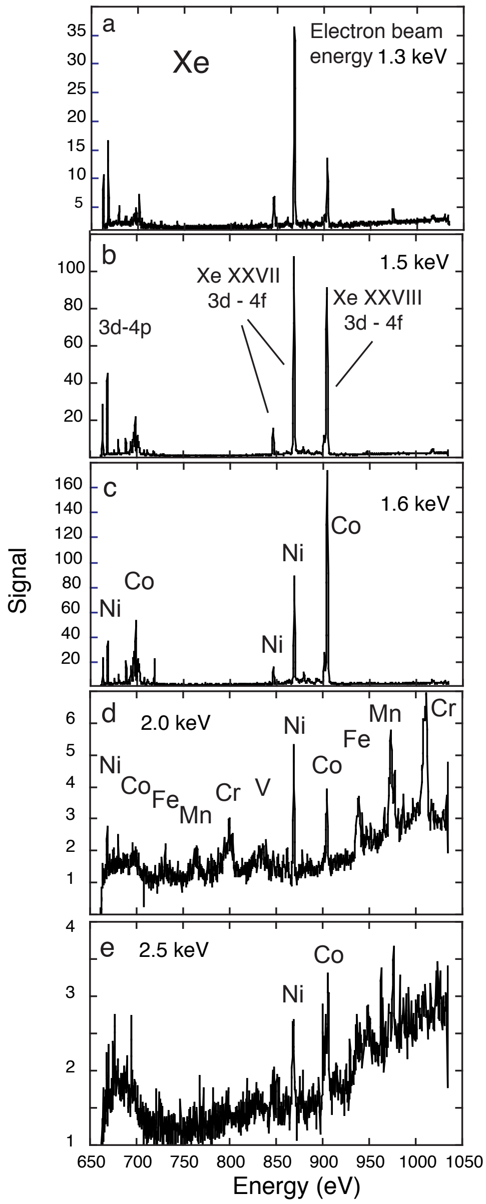

Figure 2. Spectra of Xe at various electron beam energies. (**a**) 1.3 keV, below the ionisation potential of the Ni-like ion Xe^{26+} (spectrum Xe XXVII). The lines of the Co-like ion Xe^{27+} (spectrum Xe XXVIII) can only appear after multistep ionisation has produced that charge state ion. (**b**) Electron beam energy 1.5 keV; (**c**) Electron beam energy 1.6 keV, just above the ionisation energy of the Ni-like ion Xe^{26+}. Xe^{27+} is prominently produced. (**d**) Electron beam energy 2.0 keV, which is high enough to produce Xe^{32+} (Ti-like) ions. Both, 3d-4p and 3d-4f, line series representing the ions Xe^{26+} to Xe^{31+} appear. Note the much lower signal rate than in the previous spectra. (**e**) Electron beam energy 2.5 keV, high enough to produce Xe^{36+} (Ar-like) ions (but that is outside the spectral range of this measurement). The lower charge states apparently have largely burned out.

Structure Computations

The structure of Ni-like ions has been calculated by a number of different algorithms. Biémont and Quinet [16,17] have treated Ni-like ions, but only a few and far apart ones, and not those of Xe among them, or not the *M*3 decays. Safronova et al. have repeatedly calculated transitions in Ni-like ions using relativistic many-body perturbation theory codes. In their earlier papers [18,19], the $3d^9 4s$ levels or the *M*3 decay were not treated, and calculations of the *M*3 transition energies were only executed upon request [20]. The FAC computations by Gu [21] of Ni- and Co-like ions (see [5]) concentrate on a few elements, but they could easily be extended to others, with a level of accuracy that is competitive with that achieved by traditionally "larger" codes.

The latest large-scale presentation of calculational results from relativistic many-body perturbation theory (RMBPT) computations for Ni-like ions by Safronova et al. [22–24] proceed from the level structure to higher multipole order transition rates (including the $M3$ transition rates). Safronova et al. [23] include $\Delta n = 0$ transition rates involving $3s^2 3d^9 4l$ and $3s3d^{10}4l$ levels, an addition which indicates how many more levels (with inner excitations) ought to be considered and that the present level sample in Figure 1 represents just a (prominent) fraction thereof. Since hyperfine effects in Ni-like ions have been recognised to affect the metastable level lifetime, the spectrum of computations has expanded again, far beyond the horizon of the present study.

Of specific importance in the present context are two publications by the Safronovas and Beiersdorfer [23,24]. The first of these papers indicates that many of the 4d levels have lifetimes on the order of picoseconds, related to the $E1$ decays to 4p levels (transition rates on the order of $10^{13}\,s^{-1}$). The second paper presents lifetimes of $4l$ levels as computed from higher-order decays (mostly to ground) but leaving out the $E1$ decay channels. Some seemingly long-lived levels listed in the second paper actually are not long-lived at all, because only the combination of the two computations yields the true picture. A rough estimate indicates that for seemingly long-lived 4d levels (long-lived only when consulting only the tabulation of higher-multipole order transition rates) the intra-shell $E1$ decay rate dominates the total decay rate by several orders of magnitude (for some levels by many orders of magnitude). This relation supports the observations and their interpretations presented below.

4. Observations

The spectra measured in the present context have been condensed into Figure 2. In order to prevent optical clutter, some of the labelling has been distributed over the individual plots, but not repeated for all of those in which the features are present. The 3d-4p transitions in Ni- and Co-like ions (with photon energies below some 720 eV) have been described elsewhere [5,7]. The ionisation potential of the Ni-like ion Xe^{26+} is close to 1500 eV, which is why below that electron beam energy no Co-like Xe^{27+} should be produced. However, due to stepwise ionisation involving the metastable level, electrons of 900 eV and higher can effect ionisation of Ni-like ions in the $3d^9 4s\ ^3D_3$ state.

The result of this situation can be seen in Figure 2a, a spectrum recorded at an electron beam energy of 1300 eV. Both, the 3d-4p and the 3d-4f line groups, show that Co-like ions are present, but there are clearly fewer of those ions than of Ni-like ions. The comparison is easiest for the 3d-4f transitions with their few lines from $E1$ transitions. Their transition rates are relatively high (the actual values do not matter here), so that the photon signal should represent (approximately) the relative abundances. At an electron beam energy of 1500 eV (Figure 2b), a certain fraction of electrons in the beam may still be below the ionisation threshold, while the others are at or above threshold, the abundance difference is smaller.

At an electron beam energy of 1600 eV (Figure 2c), all beam electrons can ionise Ni-like Xe ions from the ground state. The line ratios show that the charge state distribution has now shifted to Co-like ions as the majority species. The ionisation potential of Co-like ions amounts to about 1571 eV [11]. The line signal level is highest among the samples of Figure 2. No signal from higher charge states is present.

At an electron beam energy of 2000 eV (Figure 2d) the situation has changed drastically. Higher charge states are reached, and thus the signal from Ni- and Co-like ions is much reduced. On the high-energy side of, both, the 3d-4p and the 3d-4f lines, new line groups appear that by their distance from the reference lines and their regular spacing suggest identification with similar transitions in Fe-like ions (IP 1653 eV), Mn-like ions (IP 1742 eV), Cr-like ions (IP 1826 eV), and V-like ions (IP 1919 eV). The charge state distribution is much wider than before, and thus the observed lines must be weaker individually. Here it suddenly matters that no 3d-4d lines are seen from Ni- and Co-like ions - the view is free to observe the 3d-4s and 3d-4p lines of higher charge states.

At an electron beam energy of 2500 eV (Figure 2e) it should be possible to produce ions up to Ar-like (IP 2556 eV), for which ions the X-ray signal of 3d-4p and 3d-4f lines should fall beyond the spectral energy range presently covered. Moreover, the "lower charge state" ions (prominent in Figure 2d) would largely have burned out, which fits to the observation in this spectrum.

5. Discussion

Figure 2d demonstrates that as a function of electron beam energy, signals from a range of charge states can be obtained simultaneously. This would allow to study the evolution of charge state distributions fairly simply and quickly on the basis of multi-channel EUV or soft-X-ray spectra. Amusingly, a key feature is not seen in the spectra: It is exactly the non-observation of 3d-4d transitions in Ni- and Co-like ions that enables these useful observations, because this fact leaves a window in the spectrum that is not populated by prominent transitions of other origins. Instead of the 3d-4d transitions (their possible intensity is "diverted" towards 4p-4d transitions of much higher transition rates, a scenario that is supported by the aforementioned computations performed by Safronova, Safronova and Beiersdorfer [23,24]). In the spectrum gap a series of line clusters appears: progressions of 3d-4p lines from higher charge state ions, and similarly 3d-4f line clusters in the adjacent higher photon energy interval.

It is interesting to see computational efforts successfully delivering the rates of higher multipole order transitions than $E1$ in the 3d-4ℓ transition manifold. This impressive body of computational results is important for complete spectrum and level population models. However, the present example shows that a single, simple fact may be of mere practical importance, that is, no 3d-4d $E1$ transitions are allowed (they are forbidden by parity), and thus, incidentally, something else that is of plasma diagnostic interest can be observed in the same wavelength range (a "spectral window" of observational convenience) instead. In the present experiment, the 3d-4s, 3d-4p, and 3d-4f lines from higher charge state ions were seen without obstruction when the electron beam energy of EBIT-I was raised.

Funding: This research received no external funding. The APC was partly funded by Ruhr-Universität Bochum.

Data Availability Statement: The research data are available from the author upon reasonable request.

Acknowledgments: ET happily acknowledges the dedicated technical support by Ed Magee, Merv Lawrence, and Phil D'Antonio as well as the laboratory collaboration with Peter Beiersdorfer, Greg V. Brown, Hui Chen, and Mark May. ET acknowledges travel support by the German Research Association (DFG). The experimental work at the University of California Lawrence Livermore National Laboratory was performed in 2006 under the auspices of the Department of Energy under Contract No. W-7405-Eng-48.

Conflicts of Interest: The author declares no conflicts of interest.

References

1. Beiersdorfer, P.; Osterheld, A.L.; Scofield, J.; Wargelin, B.; Marrs, R.E. Observation of magnetic octupole decay in atomic spectra. *Phys. Rev. Lett.* **1991** *67*, 2272–2275. [CrossRef]

2. Träbert, E.; Beiersdorfer, P.; Brown, G.V.; Boyce, K.R.; Kelley, R.L.; Kilbourne, C.A.; Porter, F.S.; Szymkowiak, A. Time-resolved soft-x-ray spectroscopy of a magnetic octupole transition in nickel-like xenon, cesium, and barium ions. *Phys. Rev. A* **2006**, *73*, 022508. [CrossRef]
3. Träbert, E.; Beiersdorfer, P.; Brown, G.V. Observation of hyperfine mixing in measurements of a magnetic octupole decay in isotopically pure nickel-like ^{129}Xe and ^{132}Xe Ions. *Phys. Rev. Lett.* **2007**, *98*, 263001. [CrossRef] [PubMed]
4. Beiersdorfer, P.; Magee, E.W.; Träbert, E.; Chen, H.; Lepson, J.K.; Gu, M.-F.; Schmidt, M. Flat-field grating spectrometer for high-resolution soft x-ray and extreme ultraviolet measurements on an electron beam ion trap. *Rev. Sci. Instrum.* **2004**, *75*, 3723–3726. [CrossRef]
5. Träbert, E.; Beiersdorfer, P.; Gu, M.F. Spectra of Ni- and Co-like ions of Xe in an electron-beam ion trap. *Can. J. Phys.* **2008**, *86*, 467–475. [CrossRef]
6. Träbert, E. Differential observations in spectroscopic measurements using electron beam ion traps. *J. Phys. B At. Mol. Opt. Phys.* **2009**, *42*, 154019. [CrossRef]
7. Träbert, E.; Gu, M.F.; Hansen, S.B. Metastable level in Ni-like ions and time-resolved extreme-ultraviolet observation of Xe ions in an electron beam ion trap. *Phys. Rev. E* **2025**, *112*, 065210. [CrossRef]
8. Burke, T.; Takacs, E.; Dipti; Hosier, A.; O'Neil, G.; Tan, J.; Staiger, H.; Naing, A.; Marler, J.; Ralchenko, Y. High resolution X-ray spectra of the time evolution of emission from metastable electronic states of highly charged Ni-like ions. *Eur. Phys. J. D* **2024**, *78*, 78. [CrossRef]
9. Faiyaz, C.A.; Takacs, E.; Burke, T.; Dipti; O'neil, G.C.; Hosier, A.; Staiger, H.; Tan, J.N.; Ralchenko, Y. Impact of Ni-like metastable states and hyperfine quenching on charge state distribution in an EBIT. *J. Instrum.* **2025**, *20*, C06068. [CrossRef]
10. Levine, M.A.; Marrs, R.E.; Bardsley, J.N.; Beiersdorfer, P.; Bennett, C.L.; Chen, M.H.; Cowan, T.; Dietrich, D.; Henderson, J.R.; Knapp, D.A.; et al. The use of an electron beam ion trap in the study of highly charged ions. *Nucl. Instrum. Meth. B* **1989**, *43*, 431–440. [CrossRef]
11. Kramida, A.; Ralchenko, Y.; Reader, J.; NIST ASD Team. NIST Atomic Spectra Database (Ver. 5.12). 2024. Available online: https://physics.nist.gov/asd (accessed on 1 July 2024).
12. Porter, F.S.; Audley, M.D.; Beiersdorfer, P.; Boyce, K.R.; Brekosky, R.P.; Brown, G.V.; Gendreau, K.C.; Gygax, J.; Kahn, S.; Kelley, R.L.; et al. Laboratory astrophysics using a spare XRS microcalorimeter. *Proc. SPIE* **2000**, *4140*, 407.
13. Porter, F.S.; Brown, G.V.; Boyce, K.R.; Kelley, R.L.; Kilbourne, C.A.; Beiersdorfer, P.; Chen, H.; Terracol, S.; Kahn, S.M.; Szymkowiak, A.E. The Astro-E2 X-ray spectrometer/EBIT microcalorimeter x-ray spectrometer. *Rev. Sci. Instrum.* **2004**, *75*, 3772–3774. [CrossRef]
14. Porter, F.S.; Gygax, J.; Kelley, R.L.; Kilbourne, C.A.; King, J.M.; Beiersdorfer, P.; Brown, G.V.; Thorn, D.B.; Kahn, S.M. Performance of the EBIT calorimeter spectrometer. *Rev. Sci. Instrum.* **2008**, *79*, 10E307. [CrossRef]
15. Chen, H.; Beiersdorfer, P.; Fournier, K.B.; Träbert, E. Soft-x-ray spectra of highly charged Kr ions in an electron beam ion trap. *Phys. Rev. E* **2002**, *65*, 056401. [CrossRef]
16. Biémont, E. Multipole transitions in nickel-like and palladium-like spectra. *J. Phys. B At. Mol. Opt. Phys.* **1997**, *30*, 4207–4222. [CrossRef]
17. Quinet, P.; Biémont, E. Transition rates and wavelengths in the X-ray spectra of Nickel-like ions (Ag XX-Pb LV). *Phys. Scr.* **1991**, *43*, 150–157. [CrossRef]
18. Safronova, U.I.; Johnson, W.R.; Albritton, J.R. RMB calculations of excitation energies and oscillator strengths in Ni-like ions. *Phys. Rev. A* **2000**, *62*, 052505. [CrossRef]
19. Hamasha, S.M.; Shlyaptseva, A.S.; Safronova, U.I. E1, E2, M1, and M2 transitions in the nickel isoelectronic sequence. *Can. J. Phys.* **2004**, *82*, 331–356. [CrossRef]
20. Träbert, E.; Beiersdorfer, P.; Brown, G.V.; Terracol, S.; Safronova, U.I. Atomic spectroscopy of trapped, highly charged, heavy ions. *Nucl. Instrum. Meth. Phys. Res. B* **2005**, *235*, 23–27. [CrossRef]
21. Gu, M.F. The flexible atomic code. *Can. J. Phys.* **2008**, *86*, 675–689. [CrossRef]
22. Safronova, U.I.; Safronova, A.S.; Hamasha, S.M.; Beiersdorfer, P.B. Relativistic many-body calculations of multipole (E1, M1, E2, M2, E3, and M3) transition wavelengths and rates between $3l^{-1}4l'$ excited and ground states in nickel-like ions. *At. Data Nucl. Data Tables* **2006**, *92*, 47–104. [CrossRef]
23. Safronova, U.I.; Safronova, A.S.; Beiersdorfer, P.B. Relativistic many-body calculations of electric-dipole lifetimes, rates and oscillator strengths of $\Delta n = 0$ transitions between $3l^{-1}4l'$ states in Ni-like ions. *J. Phys. B At. Mol. Opt. Phys.* **2007**, *40*, 955. [CrossRef]
24. Safronova, U.I.; Safronova, A.S.; Beiersdorfer, P.B. Relativistic many-body calculations of lifetimes, rates, and line strengths of multipole transitions between $3l^{-1}4l'$ states in nickel-like ions. *Phys. Rev. A* **2008**, *77*, 032506. [CrossRef]